AFRL-PR-WP-TP-2006-208

AC LOSS REDUCTION OF YBCO COATED CONDUCTORS BY MULTIFILAMENTARY STRUCTURE

Naoyuki Amemiya, Satoshi Kasai, Keiji Yoda, Zhenan Jiang, George A. Levin, Paul N. Barnes, and Charles E. Oberly

APRIL 2006

Approved for public release; distribution is unlimited.

STINFO COPY

PROPULSION DIRECTORATE
AIR FORCE RESEARCH LABORATORY
AIR FORCE MATERIEL COMMAND
WRIGHT-PATTERSON AIR FORCE BASE, OH 45433-7251

REPORT DOCUMENTATION PAGE

Form Approved
OMB No. 0704-0188

1. REPORT DATE *(DD-MM-YY)*	2. REPORT TYPE	3. DATES COVERED *(From - To)*
April 2006	Journal article postprint	07/21/2003 – 07/21/2004

4. TITLE AND SUBTITLE
AC LOSS REDUCTION OF YBCO COATED CONDUCTORS BY MULTIFILAMENTARY STRUCTURE

5a. CONTRACT NUMBER
In-House

5b. GRANT NUMBER

5c. PROGRAM ELEMENT NUMBER
61102F/62203F

6. AUTHOR(S)
George A. Levin, Paul N. Barnes, and Charles E. Oberly (Power Generation Branch (PRPG), Power Division)
Naoyuki Amemiya, Satoshi Kasai, Keiji Yoda and Zhenan Jiang (Yokohama National University)

5d. PROJECT NUMBER
3145

5e. TASK NUMBER
32

5f. WORK UNIT NUMBER
31453279

7. PERFORMING ORGANIZATION NAME(S) AND ADDRESS(ES)

Power Generation Branch (PRPG), Power Division
Propulsion Directorate
Air Force Materiel Command, Air Force Research Laboratory
Wright-Patterson AFB, OH 45433-7251

Yokohama National University

8. PERFORMING ORGANIZATION REPORT NUMBER
AFRL-PR-WP-TP-2006-208

9. SPONSORING/MONITORING AGENCY NAME(S) AND ADDRESS(ES)

Propulsion Directorate
Air Force Research Laboratory
Air Force Materiel Command
Wright-Patterson AFB, OH 45433-7251

10. SPONSORING/MONITORING AGENCY ACRONYM(S)
AFRL-PR-WP

11. SPONSORING/MONITORING AGENCY REPORT NUMBER(S)
AFRL-PR-WP-TP-2006-208

12. DISTRIBUTION/AVAILABILITY STATEMENT
Approved for public release; distribution is unlimited.

13. SUPPLEMENTARY NOTES
Published in IOP Publishers' *Superconductor Science and Technology,* 17 (2004) 1464-1471. ©2004 IOP Publishing Ltd. PAO case number AFRL/WS 04-0751, 1 September 2004.

14. ABSTRACT
Large cross-sectional aspect ratios of YBCO coated conductors leads to large magnetization loss in AC transverse magnetic field. In this work, the magnetization loss of multifilamentary YBCO coated conductors was studied experimentally. A 100 mm length of striated multifilamentary YBCO coated conductor was prepared with the conductor and filaments 10 mm wide and 0.4 mm wide, respectively. Laser ablation was used to make the sample's striations. Magnetization loss of the striated conductor and reference nonstriated conductor was measured in AC transverse magnetic fields normal to the conductor at various frequencies. Measured loss of the 100 mm striated conductor was < 9% of the measured loss of the nonstriated conductor at f = 11.3 Hz and $H/H_{cc} = 8.8$. Even though the coupling loss component increases the magnetization loss in the striated conductor, the AC loss reduction by striation is still clear at 171.0 Hz. Transverse resistance between filaments estimated by four-probe measurement was 38 for 1 m at 80 K. Estimated coupling length is much longer than the sample length at 171.0 Hz, suggesting that filaments in striated conductors are far from 'completely coupled.'

15. SUBJECT TERMS
AC losses, coated conductors, YBCO, multifilamentary

16. SECURITY CLASSIFICATION OF:			17. LIMITATION OF ABSTRACT:	18. NUMBER OF PAGES	19a. NAME OF RESPONSIBLE PERSON (Monitor)
a. REPORT	b. ABSTRACT	c. THIS PAGE			Dr. Paul N. Barnes
Unclassified	Unclassified	Unclassified	SAR	14	19b. TELEPHONE NUMBER *(Include Area Code)* (937) 255-6241

Standard Form 298 (Rev. 8-98)
Prescribed by ANSI Std. Z39-18

INSTITUTE OF PHYSICS PUBLISHING SUPERCONDUCTOR SCIENCE AND TECHNOLOGY
Supercond. Sci. Technol. 17 (2004) 1464–1471 PII: S0953-2048(04)83937-X

AC loss reduction of YBCO coated conductors by multifilamentary structure

Naoyuki Amemiya[1,3], Satoshi Kasai[1], Keiji Yoda[1], Zhenan Jiang[1], George A Levin[2], Paul N Barnes[2] and Charles E Oberly[2]

[1] Faculty of Engineering, Yokohama National University, 79-5 Tokiwadai, Hodogaya, Yokohama 240-8501, Japan
[2] Propulsion Directorate, Air Force Research Laboratory, 2645 Fifth Street, Wright-Patterson Air Force Base, OH 45433-7919, USA

E-mail: ame@rain.dnj.ynu.ac.jp

Received 21 July 2004, in final form 21 July 2004
Published 2 November 2004
Online at stacks.iop.org/SUST/17/1464
doi:10.1088/0953-2048/17/12/018

Abstract
The large cross-sectional aspect ratio of YBCO coated conductors leads to a large magnetization loss in an AC transverse magnetic field. In this work, the magnetization loss of a multifilamentary YBCO coated conductor was studied experimentally. A 100 mm length of striated multifilamentary YBCO coated conductor was prepared where the conductor and filaments were 10 mm wide and 0.4 mm wide, respectively. Striations in the sample were accomplished by laser ablation. The magnetization loss of this striated conductor as well as a reference non-striated conductor was measured in AC transverse magnetic fields normal to the conductor at various frequencies. The measured magnetization loss of the 100 mm striated conductor was less than 9% of the measured loss of the non-striated conductor at $f = 11.3$ Hz and $H/H_{cc} = 8.8$ ($H_{cc} = I_c/\pi w_c$; I_c: critical current, w_c: conductor width). Even though the coupling loss component increases the magnetization loss in the striated conductor, the AC loss reduction by striation is still apparent even at 171.0 Hz. The transverse resistance between filaments estimated by a four-probe measurement was 38 $\mu\Omega$ for 1 m at 80 K. The coupling length estimated using this transverse resistance is much longer than the sample length even at 171.0 Hz, suggesting that the filaments in the striated conductor are far from 'completely coupled' or 'saturated'.

1. Introduction

YBCO coated conductors are being considered as the next generation, or second generation, high temperature superconducting (HTS) wires [1–4]. Both the steady-state current carrying capacity and the associated AC losses of the conductor [5–9] are important issues for AC applications such as generators, motors, transformers, etc [10]. The AC losses of YBCO coated conductors are of particular concern due to the flat tape architecture of this conductor, which results in high aspect ratios of the superconducting layer. YBCO coated conductors are expected to be 4–10 mm wide for typical applications, whereas the thickness of the YBCO layer itself is only a few microns at most. As a superconducting thin film, the magnetization loss of the YBCO increases with increasing width when exposed to an applied AC magnetic field that is perpendicular to the film's surface [11]. Amemiya *et al* [12] also demonstrated that the total AC loss of YBCO films on single crystals, which carry an AC transport current in a synchronous AC transverse magnetic field, increases with increasing film width.

One means of reducing the AC loss of the YBCO coated conductor is to bundle and transpose several narrow widths of the tape together. However, this will entail a large number of very narrow conductors to achieve an adequate current carrying capacity and require significant engineering for fabrication.

[3] Author to whom any correspondence should be addressed.

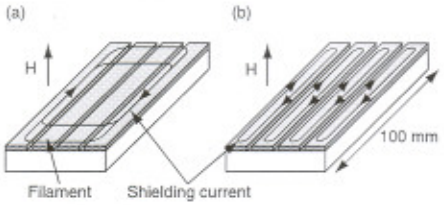

Figure 1. Shielding current induced by transverse magnetic field: (a) when filaments are completely coupled, and (b) when they are completely decoupled.

A simpler approach is to create a conductor of moderate width in which the YBCO layer consists of a filamentary structure. Carr *et al* [13] have proposed a design for a low AC loss YBCO coated conductor by subdividing the YBCO layer of the conductor into narrow filaments and then twisting the conductor as a whole. Cobb *et al* [14] have demonstrated the potential of this approach on small samples in which YBCO films were deposited on $LaAlO_3$ single crystal substrate and then subsequently striated by laser ablation. Indeed, the hysteretic loss obtained from the magnetization loops has been shown to decrease in proportion to the filament width. However, because of the low ramping rate of the applied magnetic field in these experiments, only the hysteretic loss had been measured. The coupling losses resulting from current flow between the superconducting filaments via the resistive substrate could not be detected. A finite resistance between filaments and a finite twist pitch will lead to a frequency-dependent magnetization loss characteristic [15].

The purpose of this paper is to extend this demonstration of the AC loss reduction to YBCO coated conductors of multifilamentary structure at various frequencies. The length of the sample used was 100 mm. As such, it simulates a half pitch of a multifilamentary YBCO coated conductor which has a twist pitch of 200 mm with respect to the shielding current path against the transverse magnetic field. When filaments are not decoupled, the shielding current flows across the transverse resistance between filaments and the characteristic length of the loop of the shielding current is 100 mm, as shown in figure 1(a). When filaments are completely decoupled, the shielding current flows inside each filament, as shown in figure 1(b). This choice of simulated twist pitch is just an example, being largely determined by the constraints of the experimental setup as opposed to any particular application.

It should be noted that limitations on the minimum twist pitch will exist for multifilamentary YBCO coated conductors due to their width and bend strain criteria. Even so, the simulated twist pitch and variable-frequency measurements enable us to study the AC loss characteristic of multifilamentary YBCO coated conductors, which depends on the transverse resistance between filaments. The critical currents of the samples were measured at 77 K, and the transverse resistance between filaments was measured at various temperatures to characterize the DC properties of the samples that were used in the AC loss measurements. The measured magnetization losses were compared with analytical and numerical values for a thin strip of superconductor based on the measured critical currents.

Table 1. Specifications of sample YBCO coated conductors.

	Sample NS[a]	Sample ST[a]
Striation	No	Yes
Width of conductor	10 mm	10 mm
Width of filament	N/A	400 μm
Width of groove between filaments	N/A	100 μm
Number of filaments	N/A	20
Thickness of YBCO layer	1.4 μm	
Thickness of silver protective layer	5.1 μm	
Buffer layer	Non-conducting (primarily YSZ)	
Substrate	Hastelloy	
Critical current I_c at 77 K, self-field	184 ± 3 A[a,b]	110 A[c,e]
n value at 77 K, self-field	Not determined	21[d,e]

[a] Samples, NS and ST, were cut from a longer length of YBCO coated conductor of non-uniform critical currents, end to end of 132 A; the estimated critical current of sample ST is 106 A if the cross-sectional area is taken into account. The values shown in the table are the measured values for particular sample pieces. After obtaining the two lengths, it turned out that the 184 A sample NS represents an exceptionally good piece, whereas sample ST was from a section more typical of the overall length.
[b] A more precise value of the critical current of sample NS could not be determined, because the sample was burned out during the measurement.
[c] The critical current was determined at 1×10^{-4} V m^{-1}.
[d] The n value was determined at 2×10^{-5}–1×10^{-5} V m^{-1}.
[e] The average of values determined by two V–I curves measured at both edges.

2. Sample preparation and experimental methods

2.1. Striated and non-striated samples

Specifications of the prepared striated multifilamentary sample and a reference non-striated sample are listed in table 1. Sample NS is the non-striated reference sample and sample ST is the striated sample. Both samples were pieces of a continuously processed YBCO coated conductor length that was supplied by SuperPower, Inc. The striations of sample ST were created using a laser ablation technique [14]. During ablation, the silver protective layer, YBCO layer, and buffer layer were cut through by the laser with parallel cuts. As a result, some of the ablated materials (to include substrate material) were likely redeposited in the grooves between the filaments. Redeposition of the ablated materials clearly occurred on the upper filament edges as determined by profilometry measurements, but was minimal. An image of the whole sample, with a close-up showing the filaments and grooves of sample ST, is shown in figures 2(a) and (b), respectively.

AC loss measurements were carried out with the 100 mm length samples NS and ST as well as a shorter 26.5 mm length comparison sample STs. Sample STs was taken from the 100 mm sample ST after completion of its AC loss and critical current measurements.

2.2. Critical current measurements

The critical currents of both samples, ST and NS, were measured by a standard four-probe method at 77 K, self-field.

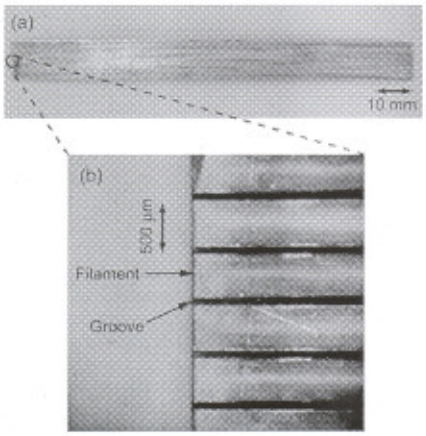

Figure 2. Striated sample: (a) image of the whole sample and (b) micrograph image of the filaments and the grooves between filaments.

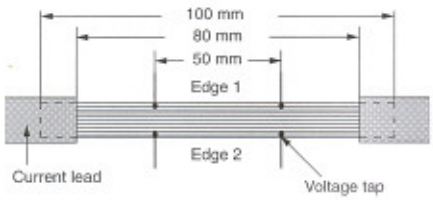

Figure 3. Sample ST and its voltage taps for critical current measurement.

The distance between the voltage taps was either 50 or 30 mm. For sample ST, the current leads were soldered at both ends, ensuring connection to all filaments. Additionally, two pairs of voltage taps were attached to each edge of the sample, as shown in figure 3; each voltage tap was attached to the two outermost filaments on each edge of the sample due to soldering size limitations. Measurement of the critical current was performed after the AC loss measurements to avoid any influence the soldering might have on the AC loss measurement. In the case of the striated sample, soldering of the current leads at both ends will definitely affect the measured AC loss, since the solder will act as an alternate interfilamentary current path.

2.3. AC loss measurements

A schematic view of the experimental setup for AC loss measurement is shown in figure 4(a) [16]. The entire system was cooled in liquid nitrogen. A 100 mm long sample was placed inside the bore of a dipole magnet that generated an AC transverse magnetic field. The sample could be rotated to vary the field orientation. The magnetization loss was measured using a linked pick-up coil (LPC) [16]; a schematic view of the LPC is shown in figure 4(b). The height and length of one turn along the sample axis, and the number of turns, are denoted by h, L, and N, respectively. The magnetization loss per unit length of the sample per cycle, Q_m, is given as

$$Q_m = C\frac{hH_{rms}V_{m,in,rms}}{NLf}, \quad (1)$$

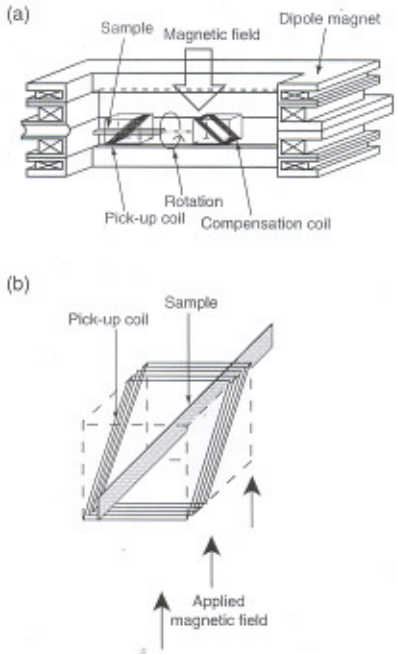

Figure 4. Experimental setup for AC loss measurements; a schematic view of (a) the entire setup and (b) the linked pick-up coil (LPC).

where C is the calibration constant of the LPC, H_{rms} is the rms of the applied magnetic field, $V_{m,in,rms}$ is the rms of the loss component of the output voltage of the LPC measured by a lock-in amplifier, and f is the frequency. The cross-sectional dimension and total length of the LPC used was 33 mm × 33 mm and 48 mm, respectively. Previous research confirmed that C is not substantially influenced by either a sample width up to 10 mm or the sample orientation. The value of C can be fixed at 2.0 for this given size of the LPC [16] when the sample is sufficiently long compared to the total length of the LPC. In the case of sample STs, which is shorter than the total length of the LPC, the measured loss was approximated using a correction factor based on the ratio between the total length of the LPC and the sample length: 48 mm/26.5 mm = 1.81.

In a series of experiments, the applied magnetic field was normal to the conductor, and the frequencies f were varied from 11.3 to 171.0 Hz.

2.4. Transverse resistance measurements

Additional samples consisting of 4 mm pieces cut from sample ST, after making the AC loss and critical current measurements, were used to determine the transverse resistance between filaments. Measurement was accomplished using a four-probe method. A schematic of a sample piece is shown in figure 5. The distance between voltage taps is 4 mm, which contains eight filaments and nine grooves for the measured section. A sample piece was cooled by helium gas to various temperatures, and 10 mA of current was fed into the sample piece for measurement of the resistance.

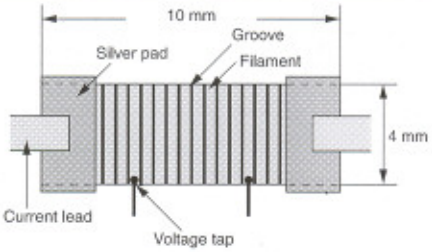

Figure 5. A sample piece for transverse resistance measurement.

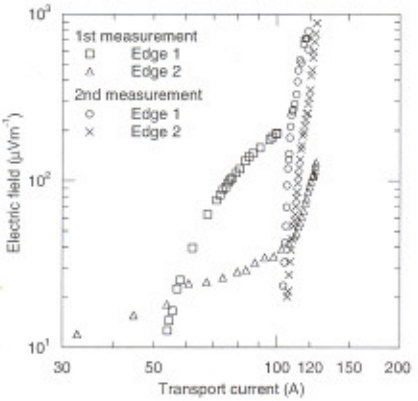

Figure 6. V–I characteristics of sample ST.

3. Experimental results and discussion

3.1. Critical current

The measured critical current I_c of sample NS was roughly 184 ± 3 A. A more precise value of I_c could not be determined, because the sample was burned out during the measurement. The measured voltage–current, V–I, characteristics of sample ST substantially depended on the contact conditions between current leads and filaments. In this case, the measured currents were the currents that were fed into the whole sample; the current distribution among filaments was unknown. In figure 6, the V–I curves measured at two edges in the first measurement attempt are shown by squares and triangles, respectively. With increasing current, a sharp increase in voltage appeared at edge 1 at approximately 50 or 60 A, while such an increase in voltage appeared at edge 2 at approximately 100 A. This result suggested poor contact resistances between the filaments and current leads; therefore, the soldering between filaments and the current leads was improved prior to the second measurement. In figure 6, the V–I curves measured at edges 1 and 2 in the second measurement are shown by circles and crosses, respectively. In the second measurement, the V–I curves measured at the two edges were similar to each other, and the critical currents were determined to be 106 and 113 A, respectively, using a 100 μV m^{-1} criterion. The average of these two values is 110 A.

Samples NS and ST were cut from a longer length of YBCO coated conductor, but were not necessarily adjacent pieces. It is particularly important to note that even though the end to end critical current was 132 A, that particular length of coated conductor was non-uniform in critical current performance. The measured critical current of 184 A of sample NS suggests that this sample represents an exceptionally good piece of the overall length. Based on the end to end I_c of 132 A and the 20% loss of YBCO cross section by striation, the I_c of a striated sample is estimated to be 106 A, which is in good agreement with the measured I_c of 110 A for sample ST. Therefore, the difference between the measured I_c of samples NS and ST does not necessarily mean any degradation in critical current during laser cutting nor any loss of filament critical current due to microstructural weak links.

3.2. AC loss in the transverse magnetic field

In figure 7, the measured AC magnetization losses Q_m of samples NS, ST, and STs are plotted against the amplitude of the transverse magnetic field $\mu_0 H_m$, where $f = 11.3$, 72.4, and 171.0 Hz. The analytical values of magnetization loss given by Brandt and Indenbom [11] and the numerical values by one-dimensional FEM analysis are also plotted in these figures.

$Q_{c,BI}$ is the analytical value per unit length of the conductor per cycle for the non-striated conductor or completely coupled striated multifilamentary conductor, and $Q_{f,BI}$ is for the decoupled striated multifilamentary conductor assuming isolated filaments:

$$Q_{c,BI} = \mu_0 w_c^2 J_{cc} t\, H g\left(\frac{H}{H_{cc}}\right), \tag{2}$$

$$Q_{f,BI} = \mu_0 w_f^2 J_{cf} t\, H g\left(\frac{H}{H_{cf}}\right) n_f, \tag{3}$$

where w_c and w_f are the conductor and filament widths, respectively, $J_{cc} = I_c/w_c t$ and $J_{cf} = I_c/w_f n_f t$ (t is the thickness of the YBCO layer and n_f is the number of filaments), $H_{cc} = I_c/\pi w_c$ and $H_{cf} = I_c/\pi w_f n_f$, and $g(x)$ is the function given by equation (4):

$$g(x) = (2/x)\ln\cosh x - \tanh x. \tag{4}$$

$Q_{f,BI}$ is the sum of the magnetization loss of isolated strip of superconductor—the influence of the neighbouring filaments is neglected. Mawatari [17, 18] calculated the magnetization of an infinite array of superconducting strips based on the critical state model and pointed out that the magnetization loss of a strip is influenced by the magnetization of neighbouring strips. Therefore, $Q_{f,BI}$ will contain an error especially when the magnetic field is small [17, 18].

Numerical electromagnetic field analysis by one-dimensional FEM [19] was made to estimate the magnetization loss in the completely decoupled samples ST and STs, where the influence of the magnetization of neighbouring filaments as pointed out by Mawatari is taken into account. The analysis was made for an array of 20 infinitely long superconducting strips as shown in figure 8. The superconducting property of the samples was represented by the power law

$$E = E_0\left(\frac{J}{J_c}\right)^n, \tag{5}$$

where the experimentally determined critical current density J_c and n value were used, and $E_0 = 1 \times 10^{-4}$ V m^{-1}. Details

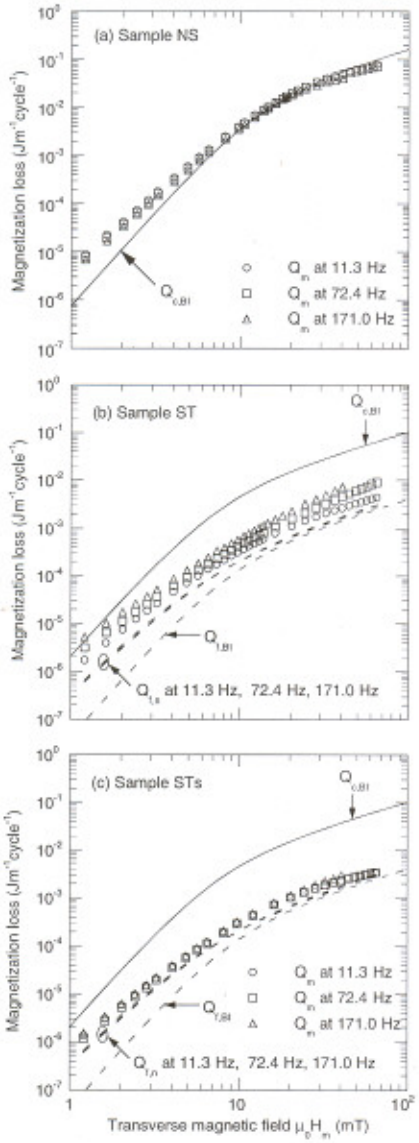

Figure 7. Measured magnetization loss Q_m, analytical magnetization loss for non-striated conductor or completely coupled striated multifilamentary conductor $Q_{c,BI}$, analytical magnetization loss for decoupled striated multifilamentary conductor assuming isolated filaments $Q_{f,BI}$, and numerically calculated magnetization loss for decoupled striated multifilamentary conductor $Q_{f,n}$ versus transverse magnetic field $\mu_0 H_m$: (a) sample NS, (b) sample ST, and (c) sample STs.

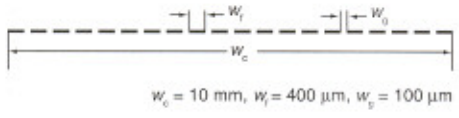

Figure 8. Cross-section of sample ST or STs for one-dimensional FEM analysis.

of the modelling are given in the appendix. Validation of the modelling was accomplished by comparing the calculated magnetization loss in an isolated solitary superconducting strip and the analytical value by Brandt and Indenbom. The numerically calculated magnetization loss is denoted by $Q_{f,n}$ in the discussion below.

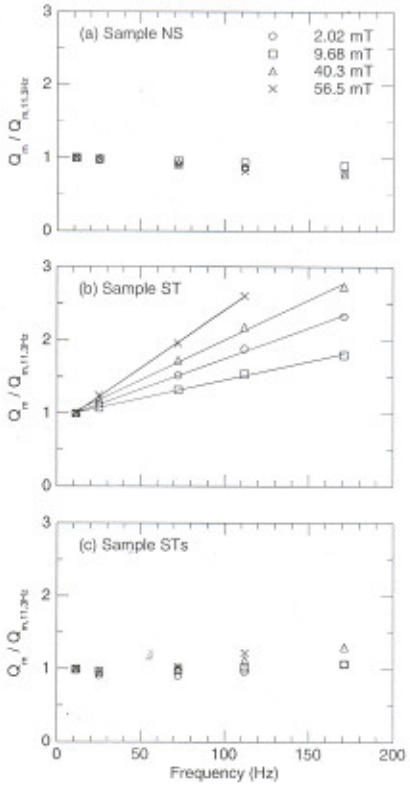

Figure 9. Magnetization losses at 2.02, 9.68, 40.3, and 56.5 mT versus frequency: (a) sample NS, (b) sample ST, and (c) sample STs. Values are normalized by magnetization loss at $f = 11.3$ Hz.

In figure 7(a), the Q_m of sample NS closely follows the analytical plot of $Q_{c,BI}$ in the large field region, although Q_m deviates from $Q_{c,BI}$ in the small field region. Such deviations have been reported previously, and one of the possible causes is a non-uniform lateral J_c distribution [6]. It is important to note that the Q_m of sample NS is almost frequency independent. The Q_m of sample ST shown in figure 7(b) is much smaller than $Q_{c,BI}$, except in the small field region which is of lesser interest from a practical point of view. Although frequency dependent, it is rather close to $Q_{f,n}$ at $f = 11.3$ Hz. The Q_m of sample STs, which is a portion of sample ST, is even closer to $Q_{f,n}$, as shown in figure 7(c). In this short sample, the frequency dependence in Q_m again disappears.

To compare the frequency dependences in Q_m for the three samples, Q_m is plotted against the frequency in figure 9. The Q_m of sample ST shown in figure 9(b) contains a substantial component which is proportional to frequency, while those of samples NS and STs are almost frequency independent. Even around 11.3 and 25.1 Hz, the Q_m of sample ST is frequency dependent. To view the frequency dependent loss component of sample ST from another perspective, the incremental changes in Q_m divided by the incremental change in frequency are plotted versus $\mu_0 H_m$ in figure 10, i.e. $(Q_{m,25.1\ Hz} - Q_{m,11.3\ Hz})/(25.1 - 11.3)$, $(Q_{m,72.4\ Hz} -$

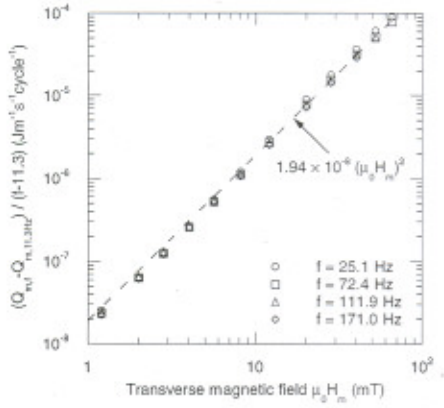

Figure 10. Incremental changes in Q_m divided by the incremental change in frequency, i.e. $(Q_{m,25.1\ Hz} - Q_{m,11.3\ Hz})/(25.1 - 11.3)$, $(Q_{m,72.4\ Hz} - Q_{m,11.3\ Hz})/(72.4 - 11.3)$, $(Q_{m,111.9\ Hz} - Q_{m,11.3\ Hz})/(111.9 - 11.3)$, and $(Q_{m,171.0\ Hz} - Q_{m,11.3\ Hz})/(171.0 - 11.3)$ versus $\mu_0 H_m$ where $Q_{m,f}$ is Q_m at f.

$Q_{m,11.3\ Hz})/(72.4-11.3)$, $(Q_{m,111.9\ Hz} - Q_{m,11.3\ Hz})/(111.9-11.3)$, and $(Q_{m,171.0\ Hz} - Q_{m,11.3\ Hz})/(171.0 - 11.3)$, where $Q_{m,f}$ is the Q_m at f. All plots collapse to one line, and the values are clearly proportional to $(\mu_0 H_m)^2$ where the proportionality coefficient is 1.94×10^{-8} where the unit of $\mu_0 H_m$ is mT. Therefore, the magnetization loss at arbitrary frequency and magnetic field can be calculated as

$$Q_{m,f} = 1.94 \times 10^{-8} (\mu_0 H_m)^2 (f - 11.3) + Q_{m,11.3\ Hz}, \quad (6)$$

where the unit of losses is J m^{-1} cycle^{-1}, and the unit of $\mu_0 H_m$ is mT. The combined observation that the frequency dependent loss component is proportional to both f and $(\mu_0 H_m)^2$ as shown in figures 9(b) and 10 strongly indicates that this loss component should either be a coupling loss of the filamentary structure or an eddy current loss in the normal conductor rather than a hysteretic loss in the superconductor.

The eddy current loss in the silver protective layer of sample ST can be calculated with the following equation given by Namjoshi and Biringer [20]:

$$Q_{e,NB} = \frac{2\pi^2 f B_m^2 J_{M,y}}{\rho_{Ag}} n_f, \quad (7)$$

where $J_{M,y} = w_f^2 t_{Ag}/12$ (t_{Ag} being the thickness of the silver protective layer) and $\rho_{Ag} = 3.0 \times 10^{-9}$ Ω m at 77 K. To properly apply this equation, $w_f/2$ must be smaller than the skin depth,

$$\delta = \sqrt{\frac{\rho}{\pi \mu_0 f}}. \quad (8)$$

Substituting 3.0×10^{-9} Ω m into ρ and 171.0 Hz into f in equation (8), δ becomes 2.1 mm, which is indeed much larger than $w_f/2$. With the appropriateness of equation (7) confirmed, $Q_{e,NB}$ is determined to be between 9.0×10^{-10} and 2.5×10^{-6} J m^{-1} cycle^{-1} for $\mu_0 H_m = 1.21$–64.5 mT, and as such is much smaller than the difference between Q_m at $f = 171.0$ Hz and $Q_{f,n}$, as shown in figure 7(b). Therefore, the frequency dependent component in the measured magnetization loss is not a result of eddy current losses due to the silver protective layer but is indeed a result of coupling losses of the filamentary structure.

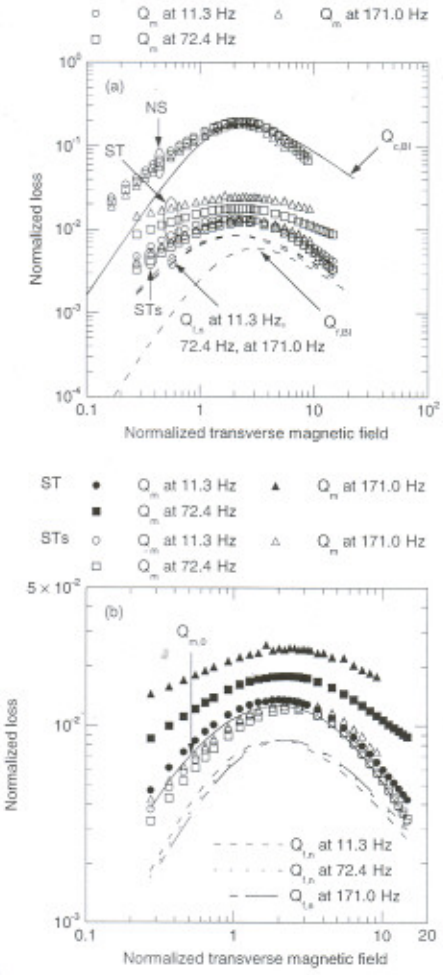

Figure 11. Normalized Q_m, $Q_{m,0}$, $Q_{c,BI}$, $Q_{f,BI}$, and $Q_{f,n}$ versus normalized magnetic field H/H_{cc} ($H_{cc} = I_c/\pi w_c$; I_c: critical current, w_c: conductor width): (a) overall view and (b) enlargement to compare the measured Q_m of samples ST and STs with $Q_{m,0}$ calculated by equation (6) and $Q_{f,n}$.

Next, we compare the measured magnetization losses of samples NS, ST, and STs to determine the effect of striation for AC loss reduction. Since the critical currents of samples NS and ST are unfortunately different, the comparison between the absolute values of their measured magnetization losses is meaningless. Here, equation (2) can be transformed to the following expression:

$$Q_{c,BI} = \frac{2B_m^2}{\mu_0} \frac{\pi w_c^2}{2} \left\{ g\left(\frac{H}{H_{cc}}\right) \Big/ \left(\frac{H}{H_{cc}}\right) \right\}, \quad (9)$$

where $B_m = \mu_0 H_m$. If $Q_{c,BI}$ is normalized by

$$\frac{2B_m^2}{\mu_0} \frac{\pi w_c^2}{2}, \quad (10)$$

and is plotted against the normalized magnetic field, H/H_{cc}, this normalized loss is independent of the critical current. This is done in figure 11(a) for the measured Q_m of samples NS, ST,

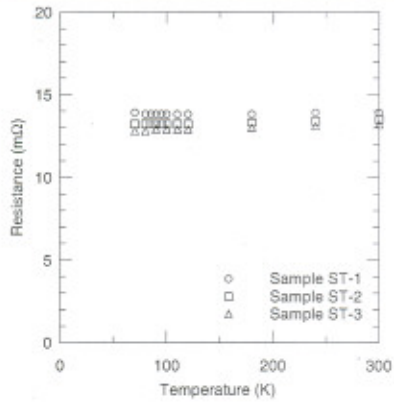

Figure 12. Transverse resistance of short pieces of sample ST as shown in figure 5 versus temperature.

and STs as well as for $Q_{c,BI}$, $Q_{f,BI}$, and $Q_{f,n}$ where $f = 11.3$, 72.4, and 171.0 Hz. Comparing $Q_{f,n}$ with $Q_{c,BI}$, it is expected that the magnetization loss should be reduced by striation to 4.3% of the value at $H/H_{cc} = 8.8$ and $f = 11.3$ Hz, while the measured magnetization losses of samples ST and STs are respectively 8.9% and 7.8% of that of sample NS at these conditions. Here, since the magnetization loss of sample ST apparently contains coupling losses even at $f = 11.3$ Hz, as shown in figures 9(b) and 10, we selected the Q_m at $f = 11.3$ Hz, where the coupling loss is minimal. One of the possible causes for the difference between the measured reduction in magnetization loss and the theoretical expectation is the assumption of uniform J_c both in the conductor as a whole and in each filament. Alternatively, at these lower applied fields, the linear proportionality of the hysteretic loss to sample width is not perfectly stringent [21]. Figure 11(b) is an enlargement of figure 11(a) to compare the measured Q_m of samples ST and STs with the $Q_{m,0}$ calculated by equation (6) and $Q_{f,n}$. $Q_{m,0}$, which is the magnetization loss of sample ST extrapolated to 0 Hz, falls around the measured Q_m of sample STs, yet is still higher than $Q_{f,n}$.

3.3. Transverse resistance

The electromagnetic coupling between filaments at a certain frequency is determined by the transverse resistance in combination with the twist pitch. The measured resistances of three short pieces of sample ST shown in figure 5 are plotted with respect to temperature in figure 12. The measured resistances are almost temperature independent. At 80 K, the average value of the measured resistances is 13.3 mΩ, while the calculated resistance of the Hastelloy substrate (4 mm wide, 4 mm long, and 100 μm thick) is 15 mΩ, assuming that the resistivity of Hastelloy is 1.5 $\mu\Omega$ m and temperature independent. The fact that the measured resistance (13.3 mΩ) is rather close to the calculated resistance of the substrate (15 mΩ) suggests that the segregated YSZ/YBCO/Ag filaments may not be connected through redeposited material with low resistivity (as a result of striating by laser ablation). As such, we will assume the electrical circuit model in the transverse direction of the striated conductor, as shown in figure 13: R_{s1} is the resistance of the

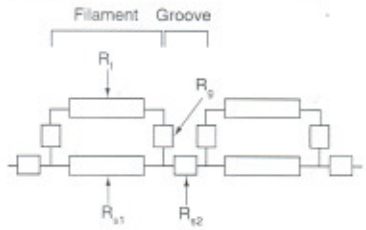

Figure 13. Electrical circuit model in the transverse direction of the striated conductor (cross-sectional view).

substrate below the filament, which is 1.5 mΩ assuming it to be 0.4 mm long, R_{s2} is the resistance of the substrate below the groove, which is 0.38 mΩ assuming it to be 0.1 mm long, and R_f is the resistance of the YSZ/YBCO/Ag layer of the filament that is zero below T_c. Then the resistance of groove R_g, which is calculated from the measured resistance of the short samples, is 4.5 mΩ, with the assumption that R_g lies between the filament and substrate, as shown in figure 13. In this model, the transverse resistance between filaments, $R_g + R_{s2} + R_g$, is 9.4 mΩ for the 4 mm of filaments (38 $\mu\Omega$ for 1 m of filaments). The transverse resistance between filaments becomes even larger, if we assume a lower value for the resistivity of Hastelloy, for example 1.4 $\mu\Omega$ m, because R_g becomes larger.

Based on this transverse resistance, a very rough estimation of the coupling length l_c is made using a simple model where two superconductor slabs are connected by a normal conductor [22]:

$$l_c = 4\sqrt{\frac{a\rho J_c}{dB/dt}}, \tag{11}$$

where a is the half width of the superconductor slab, and ρ is the resistivity of the normal conductor. If we assume that the 1.4 μm thick space in the groove between YBCO filaments is completely filled with a conducting material whose resistance is 9.4 mΩ, its resistivity ρ is 0.53 $\mu\Omega$ m. Substituting the following parameters into equation (11),

$$a = 400 \times 10^{-6}/2 = 200 \times 10^{-6} \text{ m}, \tag{12}$$

$$\rho = 0.53 \times 10^{-6} \ \Omega \text{ m}, \tag{13}$$

$$J_c = (110/20)/(1.4\times10^{-6}\times400\times10^{-6}) = 9.8\times10^{9} \text{ A m}^{-2}, \tag{14}$$

$$dB/dt = 2\pi f B_m, \qquad B_m = 50 \times 10^{-3} \text{ T}, \tag{15}$$

then l_c is 2.2, 0.86, and 0.56 m for $f = 11.3$, 72.4, and 171.0 Hz, respectively. These values are much larger than the length of sample ST (0.1 m). This estimation suggests that the filaments in sample ST are far from 'completely coupled' or 'saturated' even at 171.0 Hz. This is consistent with the observation that the Q_m of sample ST is much smaller than $Q_{c,BI}$ or the Q_m of sample NS in figures 7(b) and 11(a).

4. Conclusions

The magnetization loss of a striated multifilamentary YBCO coated conductor and that of a non-striated reference YBCO coated conductor were measured in AC transverse magnetic

fields normal to the conductor at various frequencies. The conductor and filaments were 10 mm wide and 0.4 mm wide, respectively. A substantial reduction in the magnetization loss by striation was demonstrated successfully—the measured magnetization loss of the 100 mm striated conductor was less than 9% of the measured loss of the non-striated conductor at $f = 11.3$ Hz and $H/H_{cc} = 8.8$ ($H_{cc} = I_c/\pi w_c$; I_c: critical current, w_c: conductor width). The 100 mm sample simulated a half pitch of a multifilamentary YBCO coated conductor with a twist pitch of 200 mm. The measured magnetization loss of the striated conductor contains a coupling loss component, which is proportional to the frequency and to the square of the magnetic field amplitude. The transverse resistance between filaments estimated by a four-probe measurement was 38 $\mu\Omega$ for 1 m. The estimated coupling length based on this transverse resistance is much longer than the sample length even at 171.0 Hz. This suggests that the filaments in the striated sample are far from 'completely coupled' or 'saturated'. This is consistent with the observed AC loss reduction by striation, even if the measured AC loss contains a coupling loss component. A greater reduction of AC loss at higher frequencies, mainly a reduction of the coupling loss component, is expected by increasing the transverse resistivity and/or decreasing the twist pitch. It is important to note that limitations on the minimum twist pitch of YBCO coated conductors will exist due to their width and bend strain criteria. In this regard, increasing the transverse resistivity might be a more practical means for a greater reduction of AC loss.

Acknowledgments

This work was supported by the Air Force Office of Scientific Research under contract No. AOARD-03-4031. The authors would like to thank N Enomoto of Yokohama National University for his assistance on computations of AC loss. Work by GAL was performed while holding a National Research Council Senior Research Associateship Award at the Air Force Research Laboratory.

Appendix. Electromagnetic field analysis by one-dimensional FEM [19]

Consider the temporal evolution of the current distribution in a very thin and infinitely long coated conductor. First, we define a current vector potential $\boldsymbol{T}$, where

$$J = \nabla \times T. \tag{A.1}$$

We then assume a one-dimensional model across the coated conductor. The current component normal to the conductor is neglected, and only the magnetic field component normal to the conductor is taken into account. From Maxwell's equations, the governing equation can be derived as

$$-\frac{\partial}{\partial y}\rho\frac{\partial T}{\partial y} = -\frac{\partial}{\partial t}\left(\frac{\mu_0 h}{2\pi}\int\frac{1}{y-y'}\cdot\frac{\partial T}{\partial y}\,\mathrm{d}y\right) - \frac{\partial B_0}{\partial t}, \tag{A.2}$$

where ρ is the equivalent resistivity derived from equation (5) to represent the superconducting characteristic of the coated conductor, T is the current vector potential which is normal to the conductor, h is the thickness of the conductor, and B_0 is the externally applied magnetic field component which is normal to the conductor. The first term on the right-hand side of equation (A.2) is the contribution of the self magnetic field. ρ is given as

$$\rho = \frac{E_0}{J_c}\left(\frac{J}{J_c}\right)^{n-1}. \tag{A.3}$$

A system of nonlinear equations can be obtained from equation (A.2) by the finite element method and is solved iteratively by a relaxation method.

References

[1] Watanabe T, Shiohara Y and Izumi T 2003 *IEEE Trans. Appl. Supercond.* **13** 2445–51
[2] Usoskin A, Freyhardt H C, Issaev A, Dzick J, Knoke J, Oomen M P, Leghissa M and Neumueller H W 2003 *IEEE Trans. Appl. Supercond.* **13** 2452–7
[3] Rupich M W *et al* 2003 *IEEE Trans. Appl. Supercond.* **13** 2458–61
[4] Selvamanickam V, Lee H G, Li Y, Xiong X, Qiao Y, Reeves J, Xie Y, Knoll A and Lenseth K 2003 *Physica* C **392–396** 859–62
[5] Ashworth S P, Maley M, Suenaga M, Foltyn S R and Willis J O 2000 *J. Appl. Phys.* **88** 2718–23
[6] Ogawa J, Nakayama H, Odaka S and Tsukamoto O 2004 AC loss characteristics of YBCO coated conductors with Ag protection layer *Physica* C **412–414** 1021–5
[7] Amemiya N, Jiang Z, Iijima Y, Kakimoto K and Saitoh T 2004 *Supercond. Sci. Technol.* **17** 983–8
[8] Iwakuma M, Toyoya K, Nigo M, Kiss T, Funaki K, Iijima Y, Saitoh T, Yamada Y and Shiohara Y 2004 AC loss properties of YBCO superconducting tapes fabricated by IBAD-PLD technique *Physica* C **412–414** 983–91
[9] Nishioka T, Amemiya N, Jiang Z, Iijima Y, Saitoh T, Yamada M and Shiohara Y 2004 Influence of silver-layer thickness on magnetization loss of YBCO coated conductors in transverse magnetic field with various orientations *Physica* C **412–414** 992–8
[10] Barnes P N, Rhoads G L, Tolliver J C, Sumption M D and Schmaeman K W 2004 Compact, lightweight superconducting power generators *12th Symp. on Electromagnetic Launch Technology (May 2004); IEEE Trans. Magn.* at press
[11] Brandt E H and Indenbom M 1993 *Phys. Rev.* B **48** 12893–906
[12] Amemiya N, Nishioka T, Jiang Z and Yasuda K 2004 *Supercond. Sci. Technol.* **17** 485–92
[13] Carr W J Jr and Oberly C E 1999 *IEEE Trans. Appl. Supercond.* **9** 1475–8
[14] Cobb C B, Barnes P N, Haugan T J, Tolliver J, Lee E, Sumption M, Collings E and Oberly C E 2002 *Physica* C **382** 52–6
[15] Carr W J Jr 1983 *AC Loss and Macroscopic Theory of Superconductors* (New York: Gordon and Breach) pp 106–31
[16] Jiang Z and Amemiya N 2004 *Supercond. Sci. Technol.* **17** 371–9
[17] Mawatari Y 1996 *Phys. Rev.* B **54** 13215–21
[18] Mawatari Y 1997 *IEEE Trans. Appl. Supercond.* **7** 1216–9
[19] Ichiki Y and Ohsaki H 2004 Numerical analysis of AC losses in YBCO coated conductor in external magnetic field *Physica* C **412–414** 1015–20
[20] Namjoshi K V and Biringer P P 1988 *IEEE Trans. Magn.* **24** 2181–5
[21] Sumption M D, Lee E, Cobb C B, Barnes P N, Haugan T J, Tolliver J, Oberly C E and Collings E W 2003 *IEEE Trans. Appl. Supercond.* **13** 3553–6
[22] Wilson M N 1983 *Superconducting Magnets* (Oxford: Clarendon) pp 174–5